

Circular Polarized Antenna for Radio Frequency Energy Harvesting Applications in the Smart Cities

Bujjibabu Nannepaga¹, S.Varadarajan²

¹Research Scholar, Department of ECE,

SVUCE, Sri Venkateswara University

Tirupati, Andhra Pradesh, India

e-mail: nbb.svu2020@gmail.com

² Professor, Department of ECE,

SVUCE, Sri Venkateswara University

Tirupati, Andhra Pradesh, India

e-mail: varadasouri@gmail.com

Abstract:

Objectives: In this work, the Circularly Polarized (CP) broadband antenna with a simple monopole structure is proposed. **Method:** The antenna includes the rectangular patch antenna slotted with the four arcs in a circular shape and Top-right, and down-left vertices are removed to obtain the CP and to harvest power from the frequency 1.95-3.05 GHz, it covers the LTE 2100 GHz and Wi-Fi 2.45 GHz, bands. The defected ground structure is considered to design the broadband frequency. The antenna is excited using microstrip feeding. The proposed antenna is simulated, fabricated, and measured. The Dimensions of the antenna are 45 mm x 50 mm x 1.6 mm. **Findings:** The maximum gain obtained was 4.71dB at a frequency of 2.45 GHz with a Return loss of -43.21 dB, the axial ratio (AR) obtained 1.98dB (less than 3dB) in the same frequency. The impedance bandwidth of 59.8% and 44.89% simulated and measured, respectively, at 2.45 GHz, and VSWR is 0.128 and 1.142 at 2.45 GHz for the simulated and measured, respectively. **Novelty:** The designed antenna radiation Phenomenon resembles omnidirectional characteristics. Rectenna is designed at 2.45GHz and is connected to the antenna with the help of an impedance matching network. It is used to achieve the RF- DC power conversion efficiency of 84.52%.

Keywords: Circular Polarization (CP), Radio Frequency Energy Harvesting (RFEH), Omnidirectional, Antenna.

1. INTRODUCTION

The successful implementation of several evolving technologies, including 5G systems and the internet of things (IoT), will demand the rapid increase in the usage of Wi-Fi routers, digital television transmitters, and mobile towers is not only in urban life but also in rural life, increasing energy harvesting in the ambient surroundings wirelessly [1]. Autonomous-powered IoT sensors play the leading role in extracting and monitoring information described in [2]. Advanced sensor, information, and communication technologies are the foundation of innovative city initiatives worldwide that address challenges, including air pollution, waste management, traffic optimization, and energy efficiency [3]. As a result of urbanization, smart cities are becoming a global research and development priority [4]. IoT sensors are increasingly producing vast amounts of data of many types at an unprecedented level of granularity, speed, and complexity via communication technologies, which are enormous hurdles to the research into smart cities [5],[6]. Device maintenance costs must be minimized to arrange these

sensors over a large number of network connections and carry out their activities effectively [7]. Sensors and devices equipped with sensors must be self-sufficient to fulfil this purpose. One possible method of providing them with the electricity they need is to harvest energy from natural energy sources in the environment, such as: solar, thermal, wind, mechanical and radio frequency (RF) energy [8]– [10]. Due to the rising RF energy density in metropolitan areas brought on by FM radios, mobile towers, television (TV) stations, Wi-Fi routers, and a variety of other sources, RF energy harvesting is quickly overtaking all other energy sources as the most popular technology [11]. The radio signals are absorbed by the harvesting mechanism in RFEH technology and transformed into electrical impulses appropriate for powering low-power devices [12]. This was accomplished with a device known as a Rectenna or Rectifying Antenna. The rectenna is made up of two main parts. An antenna and a rectifying circuit are involved [13]. The antenna is a front-end component of the rectenna that harvests ambient radio waves from the surrounding environment, and the rectifier converts them to direct current [14]. A compact CP antenna was

presented using a one-fourth cylindrical dielectric resonator [15]. The dumbbell shape of the slot is introduced in the ground plane to operate at the desired frequency [16]. A bow-tie-shaped planar cross dipole antenna is designed. Two bow-tie dipoles are produced on both sides of PCB and orthogonal. A novel feeding structure is used to obtain CP characteristics [17]. The CP antenna with embedded slots is designed, and a microstrip tapered feedline is used to match 50ohm impedance. It can be tested in two ways. The first way is single-source feed rectenna (SSFR), and differential source fed rectenna [18]. A novel L-slot matching antenna integrated with CP rectenna for wireless energy harvesting in the ISM band [19]. A broadband dual circular polarised DRA design using characteristic mode analysis (CMA) excited by two pairs of orthogonal degenerative modes by choosing a broadband feeding structure [20]. A low-profile Koch-Snow-flack-shaped fractal array was designed using a Wilkinson power divider to achieve CP characteristics [21].

Most reported rectennas are optimized to a fixed load but very few designs can produce a constant conversion efficiency with a varying load as we used in practice. This work investigates a CP Antenna based on single feed excitation for RFEH in smart city applications. It consists of four-arc slots in a circular shape, and antenna vertices at top-right and left-down are sliced to obtain the CP characteristics. An additional section is added to the matching network in order to maintain the good performance of the rectifier with a wide range of load, from 1 k Ω to 100 k Ω . The work in this paper will be categorised by the following sections, the brief introduction in the section 1. Methodology as section 2, in this, the proposed antenna configuration and design details are given, followed by optimisation of the antenna using the parametric analysis, finally Impedance Matching Circuit and Rectenna design were presented. In section 3, measurement results are discussed to verify the antenna performances, and the antenna is compared with some recently published antennas, followed by conclusions in section 4, finally references are in section 5.

2. METHODOLOGY

The methodology comprises of three parts Antenna geometrical representation, Parametric analysis and

impedance matching circuit and rectenna design they are elaborated given below.

i. Antenna Geometrical Representation

In this section, the schematic of the proposed antenna is presented. A rectangular Microstrip patch slotted with the four-quarter circular shape, top-right and left-down vertices is also sliced on the low-cost FR4 (Flame Retardant-4) substrate with $\text{Tan}\delta = 0.02$ and $\epsilon_r = 4.4$ has been considered. A semi-circular slot over the ground at the centre and two pairs of semi-circular patches are added symmetrically to the slot. The perspective view of the antenna is shown in Figure 1. The antenna excited using microstrip feeding. "The proposed geometry is designed first, then Optimised using Ansys HFSS v18.2 solver. The Optimised dimensions are shown in Table 1. For easy understanding, a step-by-step, optimised process has been followed for the proposed antenna that is presented in Figure 2. the performance of the antenna at different design levels is studied and illustrated graphically in Figure 3. and numerically the Table 1. To optimise the antenna, we went through four steps. In step one basic antenna is designed using the design equations; the corresponding return loss, gain, and axial ratio are plotted in figure 3. In the second step two, the radiating patch is taken as same as step one, but the ground is modified as shown in step two, and corresponding performance outcomes are plotted. Four quarter-circle slots are made on the patch without any modifications to the ground structure, and its simulated outputs are plotted. In the final step, the patch sliced at two vertices as right top and left down are as shown, and the ground is modified in three steps; step one: semi-circular slot at the top centre of the ground with a radius of 3 mm, step two: semi-circles added at the top of edges on the ground plane symmetrically with the radius of 9.06 mm. Step three: semi-circles added adjacent to the second step semi-circles of the ground plane symmetrically with the radius of 9.8 mm. all the performances of the antenna are shown in the figure, and the corresponding values are tabulated in table 2, from step one to step four return loss halved. And gain increased by a factor of 1.72. The AR decreases to 1.98 (<2).

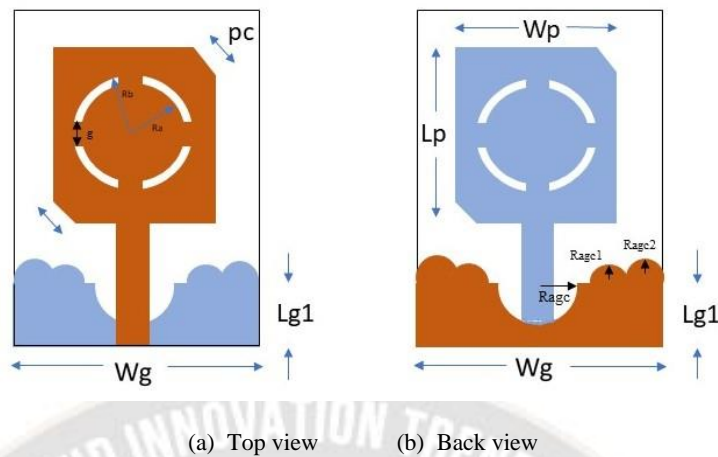


Figure 1. Proposed Antenna.

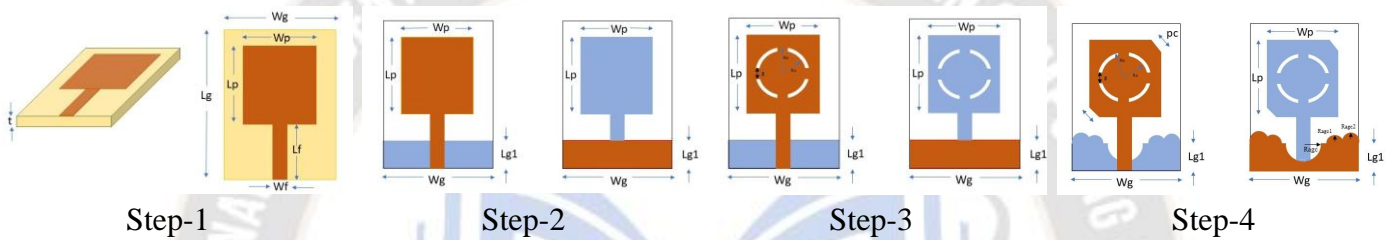


Figure 2. Antenna design Steps

Table.1.Dimensions of the optimised antenna.

Parameter	Value (mm)	Description	Parameter	Value (mm)	Description
W_g	35	Width of the Ground	R_a	9.06	The inner radius of the quarter circular-shaped arc slot
L_g	50	Lenth of the Ground	R_b	9.8	The outer radius of the quarter circular-shaped arc slot
W_p	30.06	Width of the Patch	g	4.3	The gap between the Circular arc
L_p	33.83	Lenth of the Patch	P_c	5.94	Patch cut at the Vertex
W_f	3.61	Width of the Feedline	T_{ags}	3.25	The semi-circular slot at the ground
L_f	12.88	Lenth of the Feedline	R_{agc1}	1.7	A semi-circular patch was added to the ground
t	1.5	The thickness of the Substrate	R_{agc2}	2.5	A semi-circular patch was added to the ground
L_{g1}		Length of the modified Ground	-	-	-

Table 2. Performance comparision at each design stage

Antenna performance Parameter	Frequency (GHz)	S_{11} (Return Loss) (dB)	Gain (dBi)	A.R (dB)
Antenna 1	3.184	-24.68	2.74	38.06
Antenna 2	3.184	-26.94	3.51	20.27
Antenna 3	2.176	-22.60	3.11	25.52
Antenna 4	2.45	-43.21	4.71	1.98

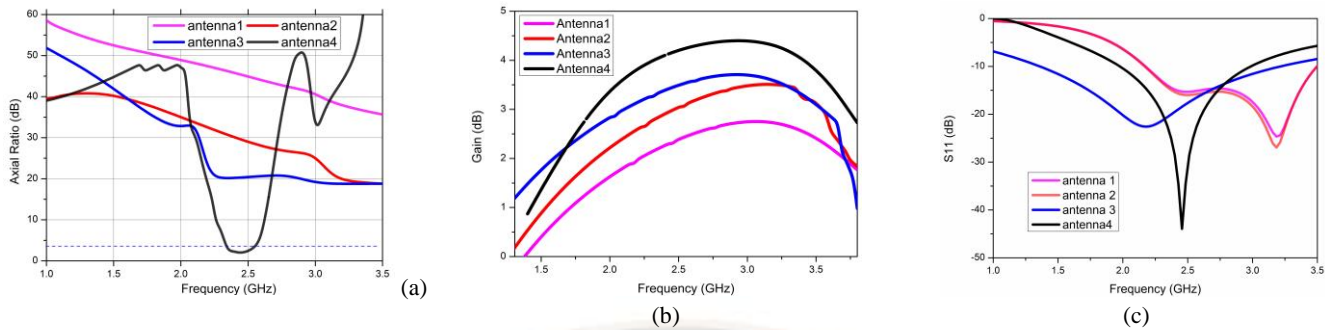


Figure 3. (a) Axial Ratio vs frequency (b). Gain vs frequency (c) S11 vs frequency

ii. Parametric Analysis

In this section, the antenna is optimised using a parametric study to find the best Optimised-dimensions of the antenna. In this connection, the variation in the antenna's gain performance and reflection coefficients are analysed with different geometrical parameters and equivalent simulated results are presented graphically.

a. Performance variation with the Width of the Transmission Line (T_{rw}):

First, the antenna transmission line length T_{rw} is varied, it is found that the width of the transmission line increases, the corresponding operating frequency decreases in the return loss plot, and there is variation in the gain plot found. The optimised width of the antenna is $T_{rw}=3.5\text{mm}$

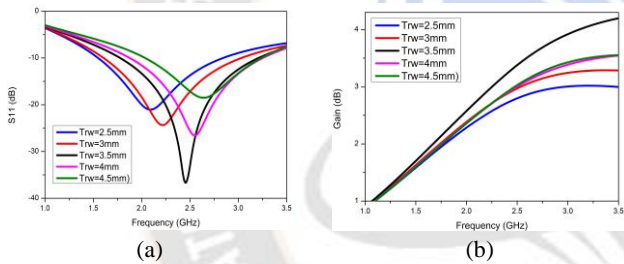


Figure 4. The Performance variation with Width of the Transmission Line (a) S11 vs Frequency (b) Gain vs Frequency

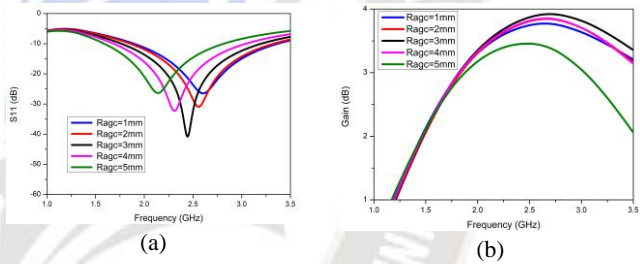


Figure 5. The performance variation with a radius of the slot on the ground (a) S11 vs Frequency (b) Gain vs Frequency

b. Performance variation with a radius of the slot on the ground (R_{sl}):

Next, the radius of the slot on the patch is analyzed on the antenna performance, and consistent outcomes are presented graphically in Figure. 3. The resonant frequency variation decreases as the slot's radius increases from 1 mm to 5 mm. Degradation in the gain performance is observed beyond 4mm. The suitable outcome achieved with $R_{sl} = 3\text{mm}$.

c. Performance variation with an inner radius of the slot on the patch (R_a):

Next, the effect of varying the inner radius of the slot on the patch was performed and presented graphically in Figure. 4. It is found that, as the inner radius increases, the resonance frequency increases up to decreases. There is a small variation in the gain performance and gain, which are inversely proportional in the range from $R_a = 4.53\text{ mm}$ to $R_a = 8.54\text{ mm}$.

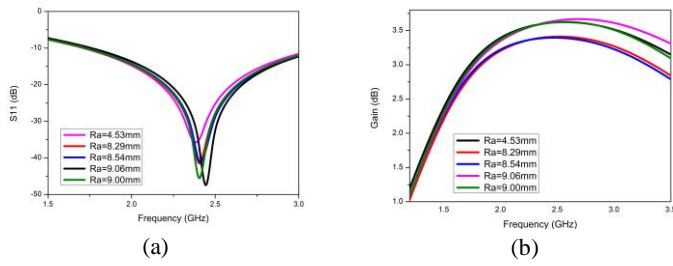


Figure 6. The performance variation with an inner radius of the slot on patch (a) S11 vs Frequency (b) Gain Vs Frequency

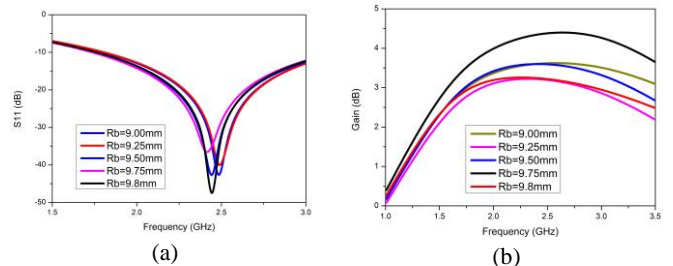


Figure 7. The performance variation with a radius of the slot on the ground (a) S11 vs Frequency (b) Gain vs Frequency

d. The performance variation with the outer radius of the slot on the patch (R_b):

Finally, the antenna was studied by changing the outer radius of the slot on the patch and respective outcomes are examined in Figure 7. It can be identified that antenna resonant frequency is inversely related to change in R_b , a considerable gain performance is observed at $R_b = 9.75$ mm optimised resonance value at $R_b = 9.8$ mm.

The optimized antenna results are plotted in Figure 8, radiation efficiency attains 97% from the frequency range 1.65 GHz to 2.55 GHz, and the axial ratio varies from 2.35 to 2.55 (<3dB) in an acceptable range. The two-dimensional antenna E-plane and H-plane patterns are simulated at 2.45 GHz frequency, and the respective results are plotted in Figure 8; it shows that the antenna exhibits omni directional properties in both the planes, and there is no significant difference is observed in E-plane and H-plane distributions. The maximum radiation pattern is present along the zero-degree direction and minimum towards

normal to its maximum direction from the E-plane pattern. The 3D radiation behaviour is shown in Figure 8. It can be found that the proposed antenna is capable of receiving radio waves from all directions in its surroundings; thus, the antenna is suitable for RFEH application in a smart city. In figure 9, shows the fabricated prototype of the antenna's top view and bottom view are shown in figure 9 (a) and (b), and measurements made using the Vector Network Analyzer (VNA).

The simulated and measured results are plotted in figure 10. The input reflection coefficient extends from 1.75 GHz to 3.2 GHz (<-10dB) and resonates at 2.45GHz with lowest value 43.21dB in the simulation range. Similarly, in measured also it is in the range of 1.95 GHz to 3.05 GHz and resonates at 2.40 GHz with the $S_{11} = -34.52$ dB. The real and imaginary impedance plots of the simulated and measured values are $Z = 49.28 + j0.007$ and $Z = 46.401 - j5.341$ respectively. The VSWR values are 0.128 and 1.142 for the simulated and measured respectively.

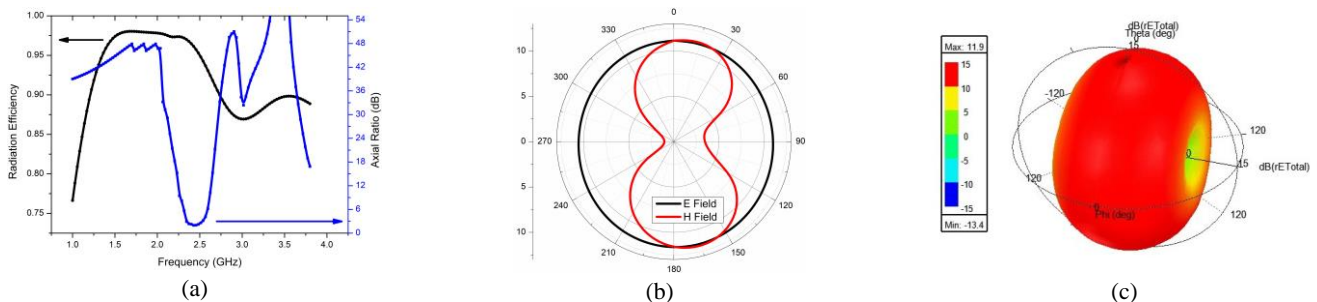


Figure 8. Optimised antenna results (a) Radiation Efficiency Vs frequency (left), axial ratio vs Frequency (right), (b) 2-Dimensional radiation pattern, (c) 3-Dimensional radiation pattern

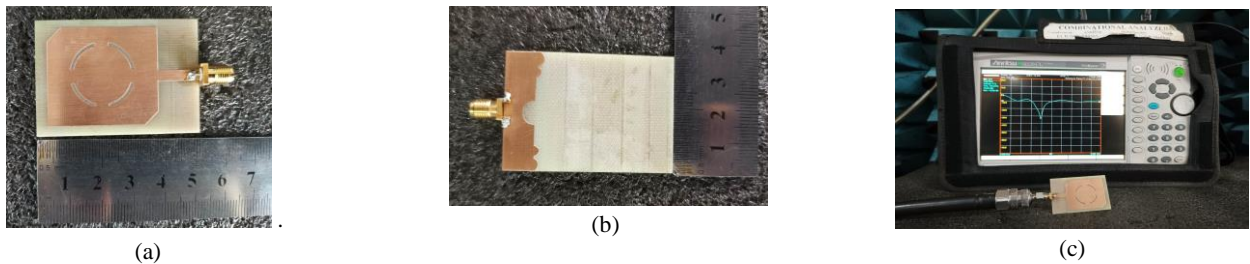


Figure 9. Fabricated antenna prototype (a) Topview (b) back view (c) Measurement of S11 using Combinational Network Analyser

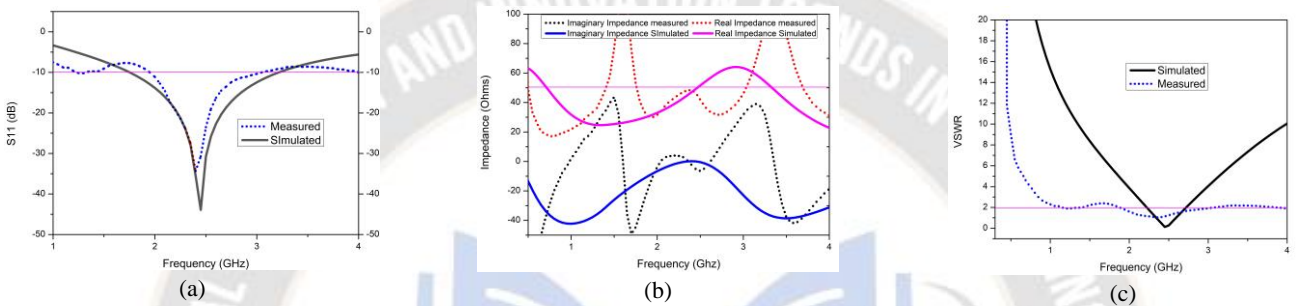


Figure 10. Measured and simulated results (a) Input reflection coefficient S11 (b) Impedance (c) VSWR

iii. Impedance Matching Circuit and Rectenna Design

The rectenna is a device used to convert Radio Frequency signal to DC signal. Rectenna is the combination of three parts antenna, impedance matching device and RF diode. The antenna collects the radio frequency signal from the free space, and the RF diode converts the RF-DC through the rectification process. An impedance matching circuit is used to match the impedance between the Antenna RF diode. Frii's equation can be used to compute the RF power harvested from free space. Frii's [17] Transmission Formula shows the link between the received and transmitted power and the free space route loss, antenna gains, and wavelength as shown in equation 1.

$$P_r = (d) \frac{G_t G_r P_t}{\left(\frac{4\pi d}{\lambda}\right)^2 L} \quad 1$$

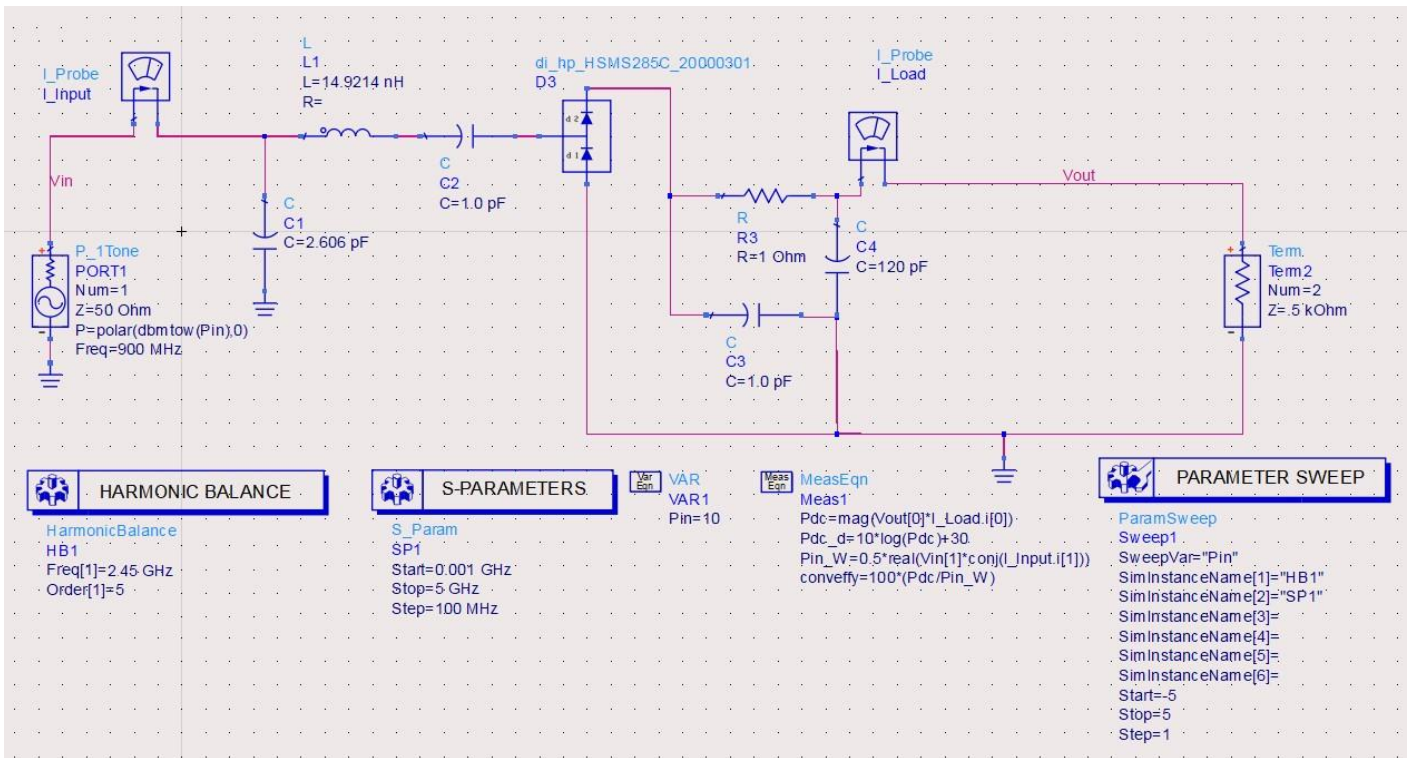
Where P_r is the received power, P_t is the transmitted power, L is the path loss factor, G_t is the transmitter antenna gain, G_r is the receiver antenna gain, λ is the wavelength, and d is the distance between the transmitter antenna and the receiver antenna.

The Schematic of the rectenna is shown in Figure 11, it consists of the following signal source (antenna), impedance

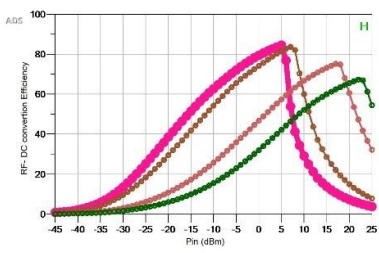
matching circuit, RF diode and finally filter. Matching of impedance between the antenna and rectifier circuit is an important factor in getting the outcome. Impedance matching is designed with the following. C_1 is the capacitor with the value of $2.606 \mu F$ and L_1 and is the inductance value 14.9214 . Impedance matching is achieved with the help of Smith Chart R_s and R_L are the source and load resistors having 50Ω and $5 K\Omega$, respectively. HSMS-285C RF diode is considered for rectification based on its electrical properties. It is designed in the Advanced Design System (ADS). Harmonic Balance Analysis is used for the simulation purpose in the conversion efficiency from the input power of -40 dBm to $+25\text{dBm}$. Load resistance R_L is varied as 500Ω , 1Ω , $5K \Omega$, and $10K\Omega$, and the corresponding RF-DC conversion Efficiency is shown in the Figureure 11 (a). The RF-DC conversion efficiency is the ratio of output DC power obtained to the received RF power; it can be calculated as

$$\eta = \frac{P_{DC}}{P_{RF}} \times 100\% \quad 2$$

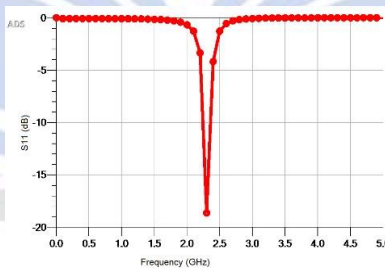
Where P_{DC} is the converted DC power from the received antenna and P_{RF} is the received RF power at the antenna terminal. The Maximum value of conversion efficiency was 84.52% obtained at the load of $5K\Omega$. The result of the S11, the lowest value is -18.5dB at 2.45GHz frequency with the $S11 < -10\text{dB}$ band value 2.35 GHz to 2.48 GHz . Plot between Pin Versus DC Output is obtained in the power range of -40 dBm to $+40 \text{ dBm}$ are shown in figure 11.



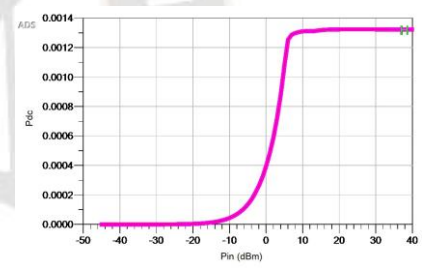
(a)



(b)



(c)



(d)

Figure 11. (a) Schematic of Rectenna, (b) RF-DC Conversion Efficiency of Rectenna, (c) Rectenna Return Loss, (d) Plot between Pin Vs. DC Output

3. RESULTS AND DISCUSSION

To verify the proposed simulation results prototype is fabricated and verified by using the Vector Network Analyzer(VNA).

Input Reflection Coefficient: S11 is the scattering parameter for the single feeding antenna. It is how much input signal is reflected when the signal is received from the same input. For any antenna, the input reflection coefficient must less the -10dB. For the optimised antenna simulated value input reflection is -43.21dB at the resonant frequency 2.45GHz.is taken from the simulation and the measured data. From the S11 we can calculate the simulated and measured impedance bandwidth for 2.45 GHz

$$\text{Simulated impedance bandwidth} = (3.2 - 1.75)/2.45 * 100\% = 59.8\%.$$

$$\text{Measured impedance bandwidth} = (3.05 - 1.95)/2.45 * 100\% = 44.89\%.$$

Voltage Standing Wave Ratio (VSWR): For the designed antenna, VSWR=0.128 and VSWR=1.142 are simulated and measured at 2.45GHz frequency, respectively. The VSWR ranges from one to infinity. For any standard antenna, VSWR must be less than two, then only it can be used for industrial and commercial purposes.

Impedance: Antenna impedance must be matched to the diode rectifier circuit. Otherwise, reflection occurs at the diode input, and then the total power received by the antenna is reflected back to the antenna at the diode. Therefore impedance matching is done at the rectifier circuit. The simulated and measured antenna impedance values are $Z=49.28+j0.007$ and $Z=46.4-j5.341$, respectively, which are very close to the 50 Ohms standard impedance value. The simulated value is with a tolerance of 1.44%, as that of the measured value.

Table 2. Comparison table of the Simulated and measured data

Performance Parameter	Frequency (GHz)	S11 (dB)	VSWR	Impedance (ohms)	Percentage of impedance bandwidth
Simulated data	2.45	-43.21	0.128	49.28+j0.00744	59.19
Measured data	2.40	-34.52	1.142	46.401-j5.341	44.89

Table 3. Comparison with the similar works

Frequency (GHz)	Antenna Dimensions (mm)	Gain (dB)	Impedance Bandwidth (GHz)	Axial Ratio Bandwidth (GHz)	Reference
2.45	40x38x7.1	4.30	2.28-2.75	2.0-2.53	[13]
2.45	160x160x1.6	4.25	2.2-2.45	2.25-2.4	[14]
2.45	π x16.3 ² x1.6	NA	2.4-2.49	2.428-2.459	[15]
2.45	30x35.5x1.6	3	2.3-2.9	2.4-2.5	[16]
2.45	70x70x0.762	5	1.7-3	1.83-2.85	[17]
5.90	28.76x28.76x0.787	6.24	5.85-5.95	5.895-5.94	[18]
2.45	45 x 50 x 1.6	4.71	1.95-3.05	2.35-2.55	This Work

We compared all the conventional design parameters that, antenna dimension, gain, impedance bandwidth and axial ratio bandwidth was able to achieved better performance of the mentioned conventional works, as shown in Table 3. It can be seen that our design seems to be the only one which can harvest energy from the ambient signals in entire band of 1.95-3.05 GHz. The measured and simulated output values are good agreement with each other. In addition, our design has a circular polarization receiving capability which can improve the overall performance. Most of the published designs are optimized to a fixed load and the conversion efficiency is heavily dependent on the varying conditions [13]-[18]. Our device has a stable performance for a wide range of load, from 1 kΩ to 100 kΩ as shown Fig. 11(b).

4. CONCLUSION

Circularly Polarized (CP) broadband antenna with a simple monopole structure is proposed which can operate from 1.95 GHz to 3.05 GHz frequency range with an AR bandwidth of 2.35 GHz - 2.55 GHz using a rectangular microstrip patch slotted with the four-quarter circular shape. The designed antenna achieve the gain of 4.71dB at 2.45 GHz frequency, which is suitable in LTE 2100 and Wi-Fi-2.45GHz Bands. It observed that simulated and measured data impedance bandwidth was 59.8% and 44.89%, respectively. The simulated and measured antenna impedance values are $Z=49.28+j0.007$ and $Z=46.4-j5.341$, respectively, which are very close to 50 Ohms standard impedance value. The simulated value has a tolerance of 0.72% as the measured value of 7.2%. The designed antenna radiation Phenomenon resembles omnidirectional characteristics. Thus the antenna can capture EM signals from all over its direction.. The Rectenna with impedance matching network was designed at

2.45 GHz frequency. The designed antenna and impedance network give good results in the same frequency. We show that with a simple yet effective design and optimization, our prototype can deliver nearly pretty good efficiency of a large commercially available energy harvesting circuit in the low incident power range simulation results for the circuit indicate roughly 84.52% operational efficiency. In conventional work, the antenna offers impedance bandwidths of 2.89 GHz (5.45–8.34 GHz) and axial ratio bandwidths of 680 MHz (5.67–6.35 GHz). There is a minimum gain of 4.8 dBi maintained by the antenna. The proposed rectenna is better than the other published designs in terms of the overall conversion efficiency as well as the coverage of frequency band and load range. It was well suited for Harvesting in the RF frequency range in smart city environments. Considering the outstanding performance of the antenna with different conditions, the proposed design is very suitable for many real-world low power devices and can therefore be applied in many battery-free wireless applications. The ambient input RF power levels as much as feasible and increase the harvesters' operational range in smart cities.

REFERENCES

- [1] C. R. Valenta and G. D. Durgin, "Harvesting Wireless Power: Survey of Energy-Harvester Conversion Efficiency in Far-Field, Wireless Power Transfer Systems," *IEEE Microw. Mag.*, vol. 15, no. 4, pp. 108–120, 2014, doi: 10.1109/MMM.2014.2309499.
- [2] G. Sun, G. Qiao, and B. Xu, "Corrosion Monitoring Sensor Networks With Energy Harvesting," *IEEE Sens. J.*, vol. 11, no. 6, pp. 1476–1477, 2011, doi: 10.1109/JSEN.2010.2100041.
- [3] B. C. Csáji, Z. Kemény, G. Pedone, A. Kuti, and J. Váncza, "Wireless Multi-Sensor Networks for Smart Cities: A Prototype System With Statistical Data Analysis," *IEEE*

- Sens. J.*, vol. 17, no. 23, pp. 7667–7676, 2017, doi: 10.1109/JSEN.2017.2736785.
- [4] G. Han, M. Guizani, J. Lloret, S. Chan, L. Wan, and W. Guibene, “Emerging Trends, Issues, and Challenges in Big Data and Its Implementation toward Future Smart Cities: Part 2,” *IEEE Commun. Mag.*, vol. 56, no. 2, pp. 76–77, 2018, doi: 10.1109/MCOM.2018.8291117.
- [5] N. Bujjibabu, S. Varadarajan, High isolated Psi-Shaped 4x4 MIMO UWB antenna for RF energy harvesting applications, *Materials Today: Proceedings*, 2023, ISSN 2214-7853, <https://doi.org/10.1016/j.matpr.2023.03.798>. Part 2,” *IEEE Commun. Mag.*, vol. 56, no. 2, pp. 76–77, 2021, doi: 10.1109/MCOM.2018.8291117.
- [6] X. Li, M. Guo, and S. Dong, “A flex-compressive-mode piezoelectric transducer for mechanical vibration/strain energy harvesting,” *IEEE Trans. Ultrason. Ferroelectr. Freq. Control*, vol. 58, no. 4, pp. 698–703, 2011, doi: 10.1109/TUFFC.2011.1862.
- [7] R. D. I. G. Dharmasena *et al.*, “Energy Scavenging and Powering E-Skin Functional Devices,” *Proc. IEEE*, vol. 107, no. 10, pp. 2118–2136, 2019, doi: 10.1109/JPROC.2019.2929286.
- [8] M. Ashraf and N. Masoumi, “A Thermal Energy Harvesting Power Supply With an Internal Startup Circuit for Pacemakers,” *IEEE Trans. Very Large Scale Integr. Syst.*, vol. 24, no. 1, pp. 26–37, Jan. 2016, doi: 10.1109/TVLSI.2015.2391442.
- [9] Y. K. Tan and S. K. Panda, “Self-Autonomous Wireless Sensor Nodes With Wind Energy Harvesting for Remote Sensing of Wind-Driven Wildfire Spread,” *IEEE Trans. Instrum. Meas.*, vol. 60, no. 4, pp. 1367–1377, 2011, doi: 10.1109/TIM.2010.2101311.
- [10] R. K. Sidhu, J. Singh Ubhi, and A. Aggarwal, “A Survey Study of Different RF Energy Sources for RF Energy Harvesting,” in *2019 International Conference on Automation, Computational and Technology Management (ICACTM)*, 2019, pp. 530–533. doi: 10.1109/ICACTM.2019.8776726.
- [11] R. J. Vyas, B. B. Cook, Y. Kawahara, and M. M. Tentzeris, “E-WEHP: A Batteryless Embedded Sensor-Platform Wirelessly Powered From Ambient Digital-TV Signals,” *IEEE Trans. Microw. Theory Tech.*, vol. 61, no. 6, pp. 2491–2505, 2013, doi: 10.1109/TMTT.2013.2258168.
- [12] D. Surender, M. A. Halimi, T. Khan, and F. A. Talukdar, “A Compact Circularly Polarized 2.45 GHz One-Fourth Cylindrical DRA for Wireless Energy Harvesting Applications in Smart City,” in *2021 IEEE Indian Conference on Antennas and Propagation (InCAP)*, 2021, pp. 739–742. doi: 10.1109/InCAP52216.2021.9726324.
- [13] C. Song *et al.*, “A Novel Six-Band Dual CP Rectenna Using Improved Impedance Matching Technique for Ambient RF Energy Harvesting,” *IEEE Trans. Antennas Propag.*, vol. 64, no. 7, pp. 3160–3171, 2016, doi: 10.1109/TAP.2016.2565697.
- [14] D. K. and K. Chaudhary, “Design of Differential Source Fed Circularly Polarized Rectenna with Embedded Slots for Harmonics Suppression,” *Prog. Electromagn. Res. C*, vol. 84, pp. 175–187, 2018, doi: 10.2528/PIERC18021401.
- [15] M. M. Mansour and H. Kanaya, “Novel L-Slot Matching Circuit Integrated with Circularly Polarized Rectenna for Wireless Energy Harvesting,” *Electronics*, vol. 8, no. 6, 2019, doi:10.3390/electronics8060651.
- [16] S. Liu, D. Yang, Y. Chen, S. Huang, and Y. Xiang, “Broadband Dual Circularly Polarized Dielectric Resonator Antenna for Ambient Electromagnetic Energy Harvesting,” *IEEE Trans. Antennas Propag.*, vol. 68, no. 6, pp. 4961–4966, 2020, doi: 10.1109/TAP.2020.2968768.
- [17] and K. S. K. Deven G. Patanvariya, Anirban Chatterjee, “High-Gain and Circularly Polarized Fractal Antenna Array for Dedicated Short Range Communication Systems,” *Prog. Electromagn. Res. C*, vol. 101, pp. 133–146, 2020, doi: 10.2528/PIERC20020706.
- [18] D. C. Hogg, “Fun with the Friis free-space transmission formula,” *IEEE Antennas Propag. Mag.*, vol. 35, no. 4, pp. 33–35, 1993, doi: 10.1109/74.229847.
- [19] Daasari Surender, Md. Ahsan Halimi, Taimoor Khan, Fazal A. Talukdar, Ahmed A. Kishk, Yahia M.M. Antar, Sembiam R. Rengarajan, Semi-Annular-Ring slots loading for broadband circularly polarized DR-Rectenna for RF energy harvesting in smart city environment, *AEU - International Journal of Electronics and Communications*, Volume 147, 2022, <https://doi.org/10.1016/j.aeue.2022.154143>.
- [20] Hao, H.; Wang, S.; Gao, H.; Ma, X.; Huang, X. Low-Cost Broadband Circularly Polarized Array Antenna with Artificial Magnetic Conductor for Indoor Applications. *Appl. Sci.* 2023, 13, 3104. <https://doi.org/10.3390/app13053104>.
- [21] Behera, B., & Mishra, S. (2022). Investigation of a high-gain and broadband circularly polarized monopole antenna for RF energy harvesting application. *International Journal of Microwave and Wireless Technologies*, 1-12. doi:10.1017/S1759078722000988.